ELASTO-PLASTIC RESPONSE OF IDEALIZED MULTI-STORY STRUCTURES SUBJECTED TO A STRONG MOTION EARTHQUAKE

Joseph Penzien*

SYNOPSIS

Presented are the results of an analytical investigation involving idealized multi-story structures subjected to the ground motion as measured by the U. S. Coast and Geodetic Survey during the May 1940 El Centro, California, earthquake. Idealized elasto-plastic resistance-deformation relationships are assumed for each structure. The basic parameters varied in the investigation are the fundamental natural period of vibration, ultimate or yield strength, and damping. All results are presented in the form of graphs showing the maximum dynamic response of each story in these structures during the simulated earthquake input plotted against the fundamental period for various combinations of ultimate strength and damping.

INTRODUCTION

The dynamic response of structures to strong motion earthquakes has been an area of research receiving much attention in recent years; thus, the true dynamic behavior of structures during an earthquake has become better understood, and as a result, the philosophy of design of structures has changed appreciably.

The earlier theoretical investigations, based purely on elastic behavior, indicated the dynamic lateral forces which developed in structures during an earthquake were considerably in excess of the static lateral forces for which they were designed. However, it has been apparent by observation that little or no damage may result to some such structures during an earthquake of high intensity. This difference between the results of observation and the results of a purely elastic analysis is due to the fact the resistance-deformation and damping characteristics of the structure are not properly defined. For the conventional structure, where its stiffness, strength, and damping properties are greatly influenced by the existence of secondary structural elements such as filler walls, partitions, stairwells, etc., and are also influenced by foundation conditions, the above structural characteristics are extremely difficult to define throughout the time history of an earthquake. However, considerable progress has been made by engineers and researchers in

---

*Associate Professor of Civil Engineering, University of California, Berkeley, California.

recent years in this direction, and as a result, the true behavior of structures subjected to strong motion earthquakes is becoming more and more amenable to theoretical analysis.

It is the purpose of this paper to present the results of a spectrum analysis of idealized multi-story structures. This investigation is a continuation of the studies presented by the author in a previous paper[1]* dealing with the spectrum analysis of a single mass system. Both studies are similar to those presented by Alford, Housner, and Martel[2] except that varying degrees of plastic deformation are allowed in the structural systems. The results show quantitatively the importance of plastic deformation in limiting the response of structural systems and also show the importance of proper lateral load distribution in design.

IDEALIZED STRUCTURES

Two idealized six-story structural types were used in this general investigation which have identical static and dynamic elastic properties but differ in their strength characteristics.

A. Static and Dynamic Elastic Properties

The elastic properties of both structural types were established by making the following assumptions:

(1) All story heights are equal,

(2) floor systems are infinitely rigid,

(3) the entire mass of the structure is concentrated equally at each floor level,

(4) the lateral deformation of the structure is a shear type of distortion, i.e., all rigid floors remain parallel,

(5) the fundamental mode of vibration is triangular in shape,

(6) all structural damping present has characteristics similar to viscous damping, and

(7) no dynamic coupling due to damping exists between the various modes of vibration.

Assumptions Nos. 1, 2, and 3 are illustrated on the diagrammatic sketch of the structure shown in Fig. 1. From assumptions Nos. 2 and 4, it is evident that the total internal spring force acting on any single floor mass depends only on the displacements of that particular floor and the two adjacent floors located directly above and below.

Assumption No. 5 was made so that the characteristic inertia loading of the first mode of vibration would be exactly similar to the inverted triangular seismic loading recommended for this mass distribution by some of the more modern building codes and which is considered more realistic

*Numbers in parentheses refer to bibliography numbers.

than the more uniform type loading used in the past. This assumption requires the story spring constants (k) to have the relative values shown in Fig. 1, which are defined in terms of the first-story spring constant (k_1). All mode shapes and periods of vibration can now be evaluated and are shown in Fig. 2.

To satisfy assumptions Nos. 6 and 7, it is necessary that the relative magnitudes of the damping coefficients (c) be similar to the relative magnitudes of the story spring constants. As shown in Fig. 1, it is convenient to express these coefficients in terms of the first-story damping coefficient (c_1), which can be evaluated in terms of the total mass of the structure (M), the fundamental period of vibration (T_1), and the usual damping factor ($\lambda = c/c_c$).

B. Strength Characteristics

The strength characteristics of both structural types used in the analysis are based on an idealized elasto-plastic relationship for the behavior of each story. This relationship assumes that deformation is purely elastic up to some yield value beyond which it is purely plastic, i.e., deformation continues with no change in resistance. Upon reversal of the direction of deformation, the story becomes elastic immediately; and when this reversed deformation is continued sufficiently, pure plastic deformation will again result, etc.

The differences between the two above-mentioned structural types are the relative magnitudes of shear (Q) at which yielding takes place in the various stories. These relative yield or ultimate shear strengths are shown in Fig. 3 for all stories of both structures along with the type of loading required to initiate yielding in all stories simultaneously as the amplitude of the loading is increased. Thus, the yield strengths of all stories are defined in terms of the total weight of the structure (Mg) and the variable parameter θ, which is defined as the yield magnitude of the ratio of total base shear to total weight of the structure.

The inverted triangular type of loading associated with structural type No. 1 was previously mentioned as the type recommended by some of the more modern codes and therefore appeared to be the most logical choice for this general investigation. However, based on the results of the spectrum analysis for this type of structure, it appeared desirable to extend the studies to structural type No. 2. The loading shown for this structural type has been recommended by the Seismology Committee of the Structural Engineers Association of California and approved by the Board of Directors of the Structural Engineers Association of California. This recommendation concentrates 10 percent of the total load at the top of the structure and distributes the remaining 90 percent in an inverted triangular manner similar to that shown for structural type No. 1

METHOD OF ANALYSIS

A. Equations of Motion

To determine the dynamic response of an idealized structure to the ground motion of an earthquake, it is necessary to solve the coupled differential equations of motion of the masses. To set up these equations, consider first the equation of motion for any arbitrary floor mass (m_i) as illustrated in Fig. 4 where the quantity u_i represents the displacement of mass m_i relative to its moving base, $(u_i)_t$ represents the total displacement of mass m_i relative to a fixed reference position, u_g represents the ground displacement, Q_i represents the total shear force developed in story i (not including damping), and c_i represents the viscous damping coefficient for story i. The equation of motion of mass m_i can be written as follows:

$$m_i (\ddot{u}_i)_t + (Q_i - Q_{i+1}) + c_i (\dot{u}_i - \dot{u}_{i-1}) - c_{i+1} (\dot{u}_{i+1} - \dot{u}_i) = 0 \quad (1)$$

However,

$$(u_i)_t = u_g + u_i \quad (2)$$

Therefore, Eq. 1 can be written as

$$m_i \ddot{u}_i + (Q_i - Q_{i+1}) + c_i (\dot{u}_i - \dot{u}_{i-1}) - c_{i+1} (\dot{u}_{i+1} - \dot{u}_i) = -m_i \ddot{u}_g \quad (3)$$

This equation of motion shows that any analysis to determine the story displacement u_i can be carried out assuming a fixed base on the structure and applying a forcing function to the mass equal to the negative product of the mass times the ground acceleration.

If the response of the structure is to be determined assuming elastic behavior, the story resistance (Q_i) would simply be the product of the story elastic spring constant (k_i) times the story shear displacement ($u_i - u_{i-1}$). However, in this investigation plastic deformation is being permitted as illustrated by the idealized shear resistance-displacement relationship shown in Fig. 5 for story i where the term U_i is defined as the ratio of the true shear displacement to the yield displacement in story i (Eq. 4).

$$U_i = \frac{(u_i - u_{i-1})}{(u_i - u_{i-1})_y} \quad (4)$$

From Eq. 4, it follows that

$$(u_i - u_{i-1}) = (u_i - u_{i-1})_y U_i \quad (5)$$

and

$$(\dot{u}_i - \dot{u}_{i-1}) = (u_i - u_{i-1})_y \dot{U}_i \quad (6)$$

The displacement of mass m_i relative to its moving base can be expressed

as the algebraic sum of all story shear displacements below mass m_i as follows:

$$u_i = \sum_{r=1}^{r=i} (u_r - u_{r-1})_y \quad U_r \tag{7}$$

Thus, the acceleration of mass m_i relative to its moving base becomes

$$\ddot{u}_i = \sum_{r=1}^{r=i} (u_r - u_{r-1})_y \ddot{U}_r \tag{8}$$

Substituting Eqs. 6 and 8 into Eq. 3 gives after some rearrangement

$$m_i (u_i - u_{i-1})_y \ddot{U}_i = -m_i \ddot{u}_g + (Q_{i+1} - Q_i) - c_i (u_i - u_{i-1})_y \dot{U}_i$$

$$+ c_{i+1} (u_{i+1} - u_i) \dot{U}_{i+1} - m_i \sum_{r=0}^{r=i-2} (u_{r+1} - u_r)_y \ddot{U}_{r+1} \tag{9}$$

$$i = 2,3,4, \text{---}$$

It is necessary that the above general equation of motion (Eq. 9) be written for each lumped mass in the structure, i.e., for all values of i in the range $1 \leq i \leq n$ where n is the number of masses in the system. Thus, one obtains n simultaneous differential equations which must be solved to obtain the time history of the dimensionless shear displacement ratios U. For any specific structural type having known relative stiffnesses and damping coefficients and having a specified mass distribution, e.g., structural type Nos. 1 and 2 in Fig. 3, these equations will contain an overall structural stiffness parameter (T_1), an overall strength parameter (Φ), and the usual damping factor (λ). These are the parameters which have been varied in this general investigation for structural types Nos. 1 and 2.

B. Integration of Equations of Motion

Due to the complications imposed by allowing plastic deformation, the n simultaneous equations of motion (Eq. 9) have been solved using a step-by-step integration procedure. By this procedure the duration of the earthquake is divided into equal small intervals of time (Δ). Assuming the quantities U, $\dot{U}$, and $\ddot{U}$ are known for each story at the beginning of any interval, these same quantities are determined at the end of that interval using the so-called "mid-acceleration" method as follows:

Let $\ddot{U}_{i,b}$, and $U_{i,b}$, and $\dot{U}_{i,b}$ represent the known values of $\ddot{U}_i$, $\dot{U}_i$, and U respectively at the beginning of any time interval. The mid-interval

values of U_i and $\dot{U}_i$ ($\bar{U}_i$ and $\bar{\dot{U}}_i$, respectively) are determined for each story ($0 \leq i \leq n$) by the simple relations

$$\bar{U}_i = U_{i,b} + \dot{U}_{i,b} \tau/2 \tag{10}$$

and

$$\bar{\dot{U}}_i = \dot{U}_{i,b} + \ddot{U}_{i,b} \tau/2 \tag{11}$$

Knowing $\bar{U}_i$ and $\bar{\dot{U}}_i$ for each story i, the shear resistance terms $\bar{Q}_i$ are obtained according to the known idealized elasto-plastic relationships (Fig. 5); thus, the mid-values of $\ddot{U}_i$ ($\bar{\ddot{U}}_i$) can be obtained using Eq. 9. However, due to the nature of the last term of Eq. 9, it is necessary that these mid-values be evaluated in the following consecutive order $\bar{\ddot{U}}_1$, $\bar{\ddot{U}}_2$, $\bar{\ddot{U}}_3$, --- $\bar{\ddot{U}}_n$.

Having all mid-values or $\bar{\ddot{U}}_i$, the magnitudes of U_i and $\dot{U}_i$ at the end of the interval are determined for each story using Eqs. 12 and 13, respectively.

$$U_{i,e} = U_{i,b} + \dot{U}_{i,b}\tau + \bar{\ddot{U}}_i \tau^2/2 \tag{12}$$

$$\dot{U}_{i,e} = \dot{U}_{i,b} + \bar{\ddot{U}}_i \tau \tag{13}$$

Knowing $U_{i,e}$ and $\dot{U}_{i,e}$ for each story i, all values of $\ddot{U}_{i,e}$ are determined in a manner similar to that above for $\bar{\ddot{U}}_i$. The known end values of $U_{i,e}$, $\dot{U}_{i,e}$, and $\ddot{U}_{i,e}$ for all stories are now used as the beginning values for the next time interval. Thus, the calculations proceed through all time intervals in a similar manner. In starting the calculations at the first time interval, the initial values of U_i and $\dot{U}_i$ are considered equal to zero for all stories.

The above numerical step-by-step method of analysis was carried out for this investigation on an IBM 701 digital computer. The computer program was written so that one could obtain either the maximum dynamic response, or the complete time history of response, for each floor of a six-story structure during an earthquake input. However, because of the computer printing time involved, the complete time history of response was obtained for one case only to aid in checking the computer program.

C. Ground Motion Used in Analysis

The ground acceleration $\ddot{u}_g$ (E-W Component) measured by the U.S. Coast and Geodetic Survey during the May 18, 1940, El Centro, California, earthquake was used throughout this investigation. Fig. 7 shows this ground acceleration plotted against time.

In carrying out the numerical integration of Eqs. 9 using this ground motion, a time interval τ equal to 0.01986 seconds was used.

ANALYTICAL RESULTS

The maximum dynamic response of each story of the structure during the period of the earthquake was of primary concern in this investigation. Therefore, all results are presented by plotting a dimensionless story displacement ratio against the fundamental elastic period of vibration of the structure for various combinations of damping and yield strength. This dimensionless displacement ratio is defined as the ratio of the maximum dynamic story displacement occurring during the simulated earthquake to the elastic displacement (for the corresponding story) produced by a "1g" static lateral loading. This "1g" lateral loading is defined not as a uniform loading but as one or the other of the loadings shown in Fig. 3 for $\theta = 1.0$. It should be noted that these "1g" story displacements, as used in the denominator of the above ratio, are purely elastic, i.e., the structure is assumed to have infinite strength. Therefore, the dimensionless strength parameter θ affects only the maximum dynamic story displacement in the numerator of this ratio. The reason for defining this ratio in such a manner is so that the maximum dynamic elasto-plastic story displacements produced during the earthquake are always compared to some fixed value as the strength parameter θ is changed. Using the notation as previously defined, this ratio is equal to $\theta\,(U_i)_{max}$. The specific type of "1g" loading represented in the spectrum analysis data will be noted on all graphs by referring to its corresponding structural type (Structure Nos. 1 or 2, Fig. 3).

All basic results of the investigation are shown in Figs. 9-23. In these Figs., the dimensionless strength parameter θ ranges from 0.05 to 1.00, the stiffness parameter T_1 ranges from 0.6 to 2.4 seconds, and the damping ratio λ is generally equal to 0.05; however, in some cases, zero damping is used. The value of 0.05 was selected for this study as it appears to be a reasonable damping factor, based on experience, for many multi-story structures.

The dashed curves appearing in Figs. 9-17 represent the response of a single mass system to this same earthquake and have been taken directly from the previously mentioned paper[1] by the author.

DISCUSSION OF RESULTS

Elastic Response

The dynamic response curves shown in Fig. 9 for idealized structure No. 1 (Fig. 3) represent purely elastic response since their ordinates never exceed the strength parameter ($\theta = 1$). Therefore, the structure acts as a linear system, which can be analyzed using the mode superposition approach, i.e., the response due to any one of its natural modes of vibration (Fig. 2) can be isolated and determined separately using a generalized single mass system. The total structural response can thus be obtained by adding algebraically the responses of the structure in all of its various modes of vibration.

In correlating the elastic response data presented in Fig. 9 for idealized structure No. 1 with the elastic response data for the single story structure, it is convenient to use the characteristic loads and corresponding story displacements of the unit loading shown in Fig. 8.

This unit loading, which consists of a negative lateral force applied to each floor equal to the weight of that floor ($m_i g$), can be divided into the characteristic loadings of the six modes of vibration as shown. Using these static characteristic loadings, their corresponding elastic story displacements $(u_i - u_{i-1})_s$ can be obtained in terms of the static elastic story displacements $(u_i - u_{i-1})_y$ for the "1g" loading representing structure No. 1. These displacements are given in the table of Fig. 8. It is significant to note that the first mode story displacements produced by the unit static loading are equal to only 80.8 percent of the elastic displacements produced by the "1g" loading (structure No. 1) , while the unit load displacement of a single mass structure is, of course, equal to 100 percent of the static elastic displacement.

From Eq. 3, it is apparent the earthquake forcing function for this structure is equal to the above unit static loading multiplied by the time dependent ground acceleration ($\ddot{u}_g$) expressed in g's. Therefore, the ratio of the maximum dynamic displacement, produced during the earthquake in any particular story by any particular mode of vibtation, to the static elastic story displacement for "1g" loading may be determined as follows: First, obtain the dimensionless response ratio for the specified natural mode of vibration from the spectral response curve for a single mass system (dashed curve, Fig. 9) using a period of vibration equal to that of the specified mode. Then, multiply this ratio by the appropriate numerical value given in the table of Fig. 8 for the corresponding story and mode of vibration. Likewise, maximum response in each of the other modes may be obtained in a similar manner.

To obtain the total maximum response of each story as represented by the solid curves in Fig. 9 using mode superposition, one would have to determine the entire time history of response for each mode of vibration independently, sum these responses algebraically, and find the maximum value of this sum during the period of the earthquake. This maximum sum is, however, not the same as the sum of the maximum response ratios determined for each mode separately, as the various modes of vibration do not in general have their maximum responses occurring at the same instant of time. This latter sum, therefore, is the upper limiting value of the former assuming ideal phasing of the various modes. To illustrate this difference, the latter sum is obtained subsequently for each story of the six-story structure represented in Fig. 9 by a fundamental period (T_1) of 2.0 seconds.

(1) Using the period ratios given in Fig. 2, the periods of vibration of all modes are found to be $T_1 = 2.00$, $T_2 = 0.89$, $T_3 = 0.52$, $T_4 = 0.38$, $T_5 = 0.30$, and $T_6 = 0.25$.

(2) For these periods, the maximum dynamic response ratios as taken from the elastic response curve[1] for a single mass system are 0.35, 0.80, 2.00, 2.70, 2.30, and 3.50, respectively.

(3) Multiplying these maximum response ratios by the story displacements for corresponding modes as given in the table of Fig. 8 and summing their absolute values give 0.55, 0.46, 0.50, 0.54, 0.65, and 0.86, respectively. The absolute sum is taken rather than the algebraic sum as the displacements can be additive due to the different frequencies of the various modes.

Note: the values given in (3) above, based on maximum response of individual modes, are somewhat higher than the maximum values of total response (0.48, 0.37, 0.41, 0.45, 0.47, and 0.78) given in Fig. 9. This difference is in agreement with the above statement made to this effect. It is significant to note also that the variations of response from story to story are similar in both cases. Thus, the correlation of the multi-story and single story results of Fig. 9 are considered good. In view of these remarks, it is apparent that for the case of zero damping the contribution of higher modes of vibration to the total structural response is considerable.

The dynamic response curves shown in Fig. 10 for idealized structure No. 1 also represent purely elastic response except that viscous damping of 5 percent has been introduced into the system. It is quite apparent from these results that the relative contributions of higher modes to the total maximum response is considerably less than for the undamped case previously discussed. This decrease is to be expected as damping in the system will greatly reduce the resonant type of response but will not greatly affect the sudden transient responses. As a result, chances are considerably less that the peak responses of the various modes will occur at or near the same instant of time. Therefore, it is reasonable to expect the multi-story response curves of Fig. 10 to drop generally below the single story response curve (A). As pointed out previously, the response of this multi-story structure considering only first mode response would be 80.8 percent of that shown by the single story structure. This would seem to indicate that for periods less than about 1.2 seconds, the total multi-story response shown in Fig. 10 is primarily due to the first mode as the ordinates are approximately 80 percent of those for curve A. However, for periods greater than 1.2, effects of higher modes become apparent.

Elasto-Plastic Response

The curves in Fig. 11, for the case of no damping ($\lambda=0$) and a strength or yield parameter $\theta = 0.20$, represent almost entirely elasto-plastic response. Since there is no damping of any kind in the system until yield displacements are reached, the resonant type of response for higher modes of vibration have a chance to build up and thus contribute appreciably to the maximum dynamic response. For the structure represented by this figure, the higher modes affect primarily the 6th, 5th, and 1st stories with the 6th story generally showing greatest response. This behavior seems consistent with the results and explanation previously set forth for the purely elastic case.

It is apparent from a comparison of Figs. 9 and 11 that plastic deformations have a considerable damping effect as maximum story displacements in Fig. 11 are in general much less than those in Fig. 9 even though the strength of the structure has been greatly reduced.

Figs. 12, 13, 14, and 15 present the response data for idealized structure No. 1 having an assumed damping factor of 5 pereent and having strength ratios (θ) of 0.30, 0.15, 0.10, and 0.05, respectively. The multi-story response curves in these Figs. are generally below the single story curves which, as previously pointed out, is characteristic also of the purely elastic case (Fig. 10).

For very weak structures, large variations are noted in Figs. 12- 15 for the maximum displacements of the various stories. The larger displacements develop in the stories which show similar large displacements for the purely elastic case (Fig. 10). Since it becomes increasingly difficult to rationalize overall structural behavior as more and more plastic deformation is permitted, any attempt to explain these variations using the usual elastic normal modes of vibration would be meaningless.

Since the response of structure No. 1 as previously discussed generally shows the 6th story to be most critical, it seemed desirable to extend the general investigation to structural type No. 2 (Fig. 3). This type, as shown in the table of Fig. 3, has added strength in the upper stories with the 6th floor having the largest percentage increase.

Figs. 16 and 17 show the response of structure No. 2 for θ values of 0.10 and 0.05, respectively. These results are quite similar to those for structure No. 1 (Figs. 14 and 15) with one noticeable difference. The 6th floor response has been greatly reduced while the 1st floor response has increased somewhat. This shows that when any one story is strengthened to reduce its plastic deformation, greater plastic deformation is likely to occur elsewhere to enable the structure to absorb the energy transmitted into the system by the earthquake. This behavior also illustrates the desirability of having shear strengths in each story which increase with plastic deformation rather than remain constant as assumed for the idealized relationship shown in Fig. 5. Even though this rate of increase with deformation is relatively small, such a bi-linear resistance-displacement relationship would force the story displacements to be reasonably uniform, i.e., the energy would be more uniformly absorbed in the structure. On the other hand, if any one story should have decreasing strength with deformation, it is likely the energy transmitted to the structure by the earthquake will localize in this particular story, which may result in ultimate failure.

All response curves for structure No. 1 are presented for each story separately in figures (Figs. 18 - 23) for values of θ ranging from 0. 60 to 0.05. By comparing the curves in each of these figures, one can more easily see the effectiveness with which plastic deformation damps the structural system. As the strength parameter (θ) is decreased, the maximum dynamic response also decreases until θ reaches some optimum value at which point a further decrease in θ results in an increase of maximum response. The multi-story results presented herein are generally similar in this respect to the single mass studies[1] which show this optimum value of θ to be approximately equal to 0.3, 0.2, and 0.1 at periods of 0.3, 0.6, and 0.9 seconds, respectively. For periods greater than 0.9 seconds, the optimum value of θ is generally about 0.1 or somewhat less. After observing these spectrum results and the ground motion shown in Fig. 7, it would seem that the optimum θ for any period of vibration is approximately equal to the amplitude (expressed as a fraction of gravity) of the component of ground acceleration having this same period. Therefore, for increasing values of θ greater than this optimum value, the maximum dynamic response is due more and more to a resonant condition which builds up over an appreciable increment of time; whereas, for decreasing θ values less than this optimum, the maximum response seems to be affected more and more by the transient response resulting from separate single ground acceleration pulses.

A general interpretation of the results presented herein would indicate that a stiff structure, i.e., periods up to approximately .8 seconds for the El Centro earthquake, must be strengthened considerably over the more flexible structures in order to limit the dynamic response. This usually is the case as the stiffer structures are generally inherently stronger. The usual type building has filler walls, partitions, stairwells, etc., which considerably strengthen the structure for small displacements(3). However, since these elements also stiffen the structure greatly, one should use this increased stiffness in interpreting any dynamic response data. While the resistance-deformation characteristics of such structures may not be similar to the idealized case used herein; nevertheless, in general the effect of forcing the structure to deform beyond its ultimate capacity results in appreciable damping which limits the dynamic response. For the so-called "modern type" structure where the structural frame is not assisted by the secondary elements mentioned above, a damping factor of 5 percent as used in this investigation seems reasonable.

It is reminded that the dynamic response values presented herein are maximum values occurring during the period of the earthquake and are not final values. The permanent plastic deformations remaining at the end of the earthquake period are in general considerably less than those indicated in Figs. 9 - 23. Therefore, the maximum response values presented may be considered as upper limits only.

GENERAL CONCLUSIONS

Based on the results of this investigation using the El Centro Earthquake of May 1940, the following general conclusions are deduced:

(1) Buildings designed under present day code requirements depend a great deal on damping to limit their dynamic response during the period of a strong motion earthquake. Since much of this damping is provided by plastic deformations, it is important that structures be designed to withstand large displacements without ultimate collapse.

(2) The maximum dynamic elasto-plastic response of a structure decreases with a decrease in lateral yield strength until this strength reaches some optimum value at which point a further decrease in strength results in an increase in dynamic response.

(3) The optimum lateral strength in limiting the maximum dynamic response is of the order of .1 gravity or less for tall flexible buildings which have long periods of vibration and is of the order of .2 gravity for low stiff buildings which have short periods of vibration.

(4) Higher modes of vibration contribute appreciably to the elastic response of multi-story structures subjected to earthquakes and may also contribute appreciably to response when limited plastic deformations are permitted; thus, proper lateral load distribution for design purposes should be carefully considered.

(5) To insure a more uniform distribution of plastic deformation in multi-story structures, it is desirable

to provide structural resistance which increases with plastic deformation over some limited range.

(6) The additional damping obtained from inelastic deformations, along with the increased strength and stiffness provided by secondary components such as walls, partitions, stairwells, etc., are primarily responsible for the apparent ability of many existing structures to withstand strong-motion earthquakes.

Conclusions 2 and 3 are based on the May 1940 El Centro Earthquake and therefore may not necessarily show this same behavior for another earthquake of somewhat different characteristics.

ACKNOWLEDGMENT

The author wishes to express his appreciation to the University of California Computer Center for the use of their IBM 701 computer in carrying out the calculations in this investigation. He also wishes to thank Professor R. W. Clough for his suggestions and comments in the preparation of this paper.

REFERENCES

1. Penzien, Joseph, "Elasto-Plastic Response of a Single Mass System Subjected to a Strong-Motion Earthquake", **Structural Journal, American Society of Civil Engineers**, June 1960.

2. Alford, J. L., Housner, G. W., and Martel, R. R., "Spectrum Analyses of Strong-Motion Earthquakes", Office of Naval Research, Contract N6 ONR-244, August 1951.

3. Blume, J. A. "Structural Dynamics in Earthquake-Resistant Design", ASCE, Structural Division, Proc. Paper 1695, July 1958.

4. "United States Earthquakes", U. S. Coast and Geodetic Survey, Gov't. Printing Office, Washington, D. C.

5. Robison, E. C., "Computations on the Response of One-Mass Undamped Structures to the El Centro Acceleragraph Record", Watson Scientific Computing Lab., Columbia University, New York, New York.

6. Newmark, N. M., "Methods of Analysis for Structures Subjected to Dynamic Loading", Report to Directorate of Intelligence Headquarters, United States Air Forces, Washington, D. C., December 1950.

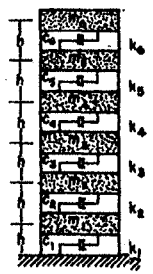

FLOOR	m_i/m_1	k_i/k_1	c_i/c_1	STORY
6	1	6/21	6/21	6
5	1	11/21	11/21	5
4	1	15/21	15/21	4
3	1	18/21	18/21	3
2	1	20/21	20/21	2
1	1	21/21	21/21	1

WHERE:

$$M = \sum_{i=1}^{6} m_i$$

$$k_1 = \frac{14\pi^2 M}{T_1^2}$$

$$c_1 = \frac{14\pi M \lambda}{T_1}$$

FIG. 1 — MASS DISTRIBUTION, SPRING CONSTANTS, AND DAMPING FACTORS, FOR IDEALIZED STRUCTURES

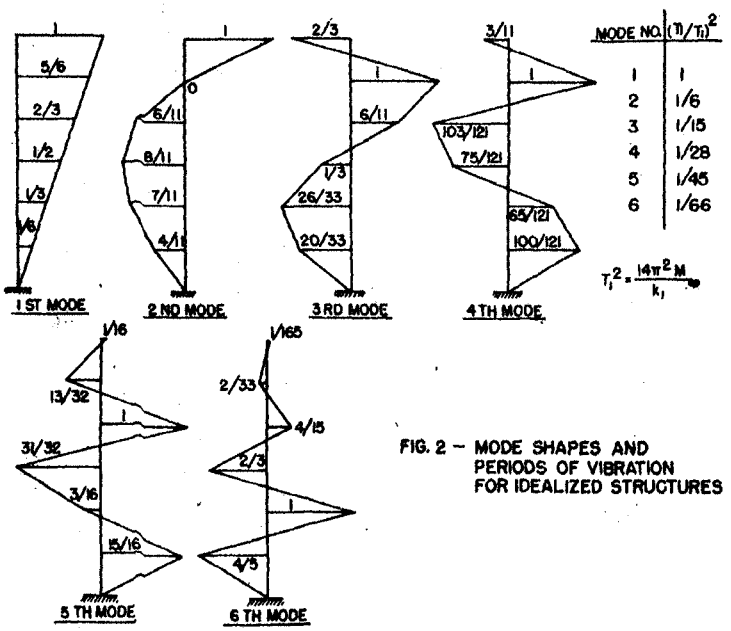

MODE NO.	$(T_1/T_i)^2$
1	1
2	1/6
3	1/15
4	1/28
5	1/45
6	1/66

$$T_i^2 = \frac{14\pi^2 M}{k_i}$$

FIG. 2 — MODE SHAPES AND PERIODS OF VIBRATION FOR IDEALIZED STRUCTURES

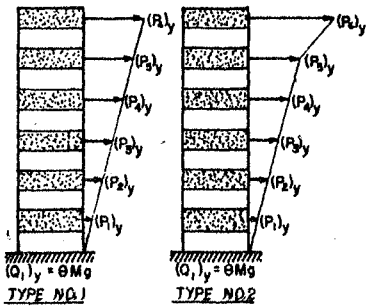

$(P_i)_y/(P_1)_y$ NO.1	NO.2	$\beta_i=(Q_i)_y/(Q_1)_y$ NO.1	NO.2	$\frac{(u_i-u_{i-1})_y}{(u_1-u_0)_y}$ NO.1	NO.2
6	8/5	12/42	15/42	1	1.2500
5	5	22/42	24/42	1	1.0909
4	4	30/42	31.2/42	1	1.0400
3	3	36/42	36.6/42	1	1.0167
2	2	40/42	40.2/42	1	1.0050
1	1	42/42	42/42	1	1.0000

$$(Q_1)_y = \sum_{j=1}^{6} (P_j)_y ; \quad (u_1-u_0)_y = \frac{(Q_1)_y}{k_1} = \frac{\theta g T_1^2}{14\pi^2}$$

FIG. 3 — STORY YIELD RESISTANCES AND CORRESPONDING YIELD DEFORMATIONS FOR IDEALIZED STRUCTURAL TYPES NOS. 1 AND 2

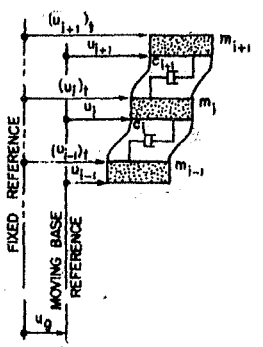

FIG. 4 — NOTATION FOR DISPLACEMENTS

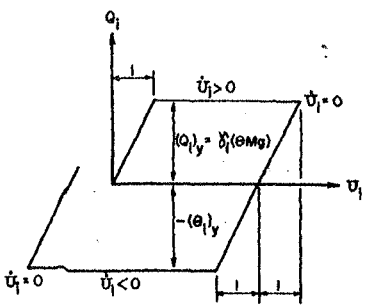

FIG. 5 — IDEALIZED ELASTO-PLASTIC SHEAR RESISTANCE DISPLACEMENT RELATIONSHIP

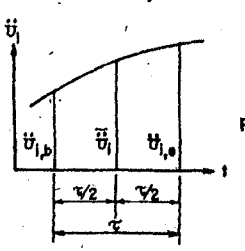

FIG. 6 — TIME INTERVAL NOTATION

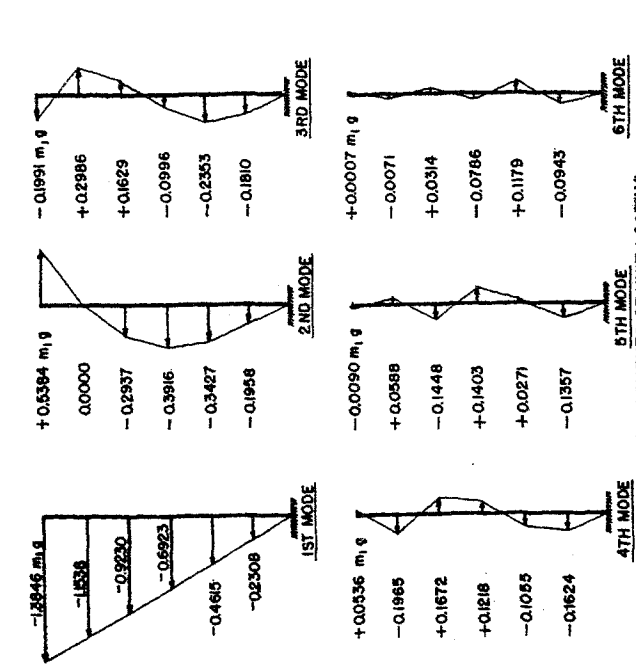

$(\ddot{u}_j - \ddot{u}_g) / (\ddot{u}_i - \ddot{u}_g)_{i=1}$; $\beta = 1.0$; STRUCTURE NO.1

STORY	MODE NO. 1	2	3	4	5	6
6	-.808	+.314	-.116	+.031	-.005	.000
5	-.808	+.171	+.032	-.046	+.016	-.002
4	-.808	+.057	+.061	+.006	-.022	+.006
3	-.808	-.029	+.032	+.028	+.009	-.010
2	-.808	-.086	-.013	+.007	+.013	+.011
1	-.808	-.114	-.042	-.020	-.011	-.005
SINGLE MASS	1.00					

COMPONENTS OF DISPLACEMENTS

FIG. 8– UNIT STATIC LOADING AND CORRESPONDING ELASTIC DISPLACEMENTS SEPARATED INTO THEIR SIX CHARACTERISTIC MODE COMPONENTS

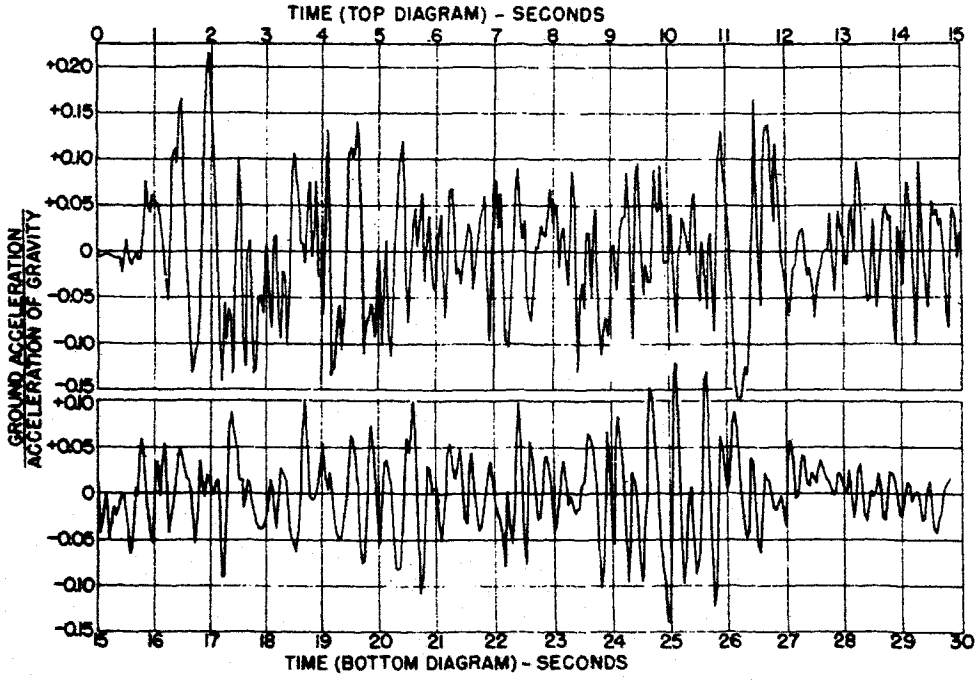

FIG. 7 -- ACCELEROGRAM FOR EL CENTRO, CALIFORNIA COMPONENT E-W EARTHQUAKE OF MAY 18, 1940

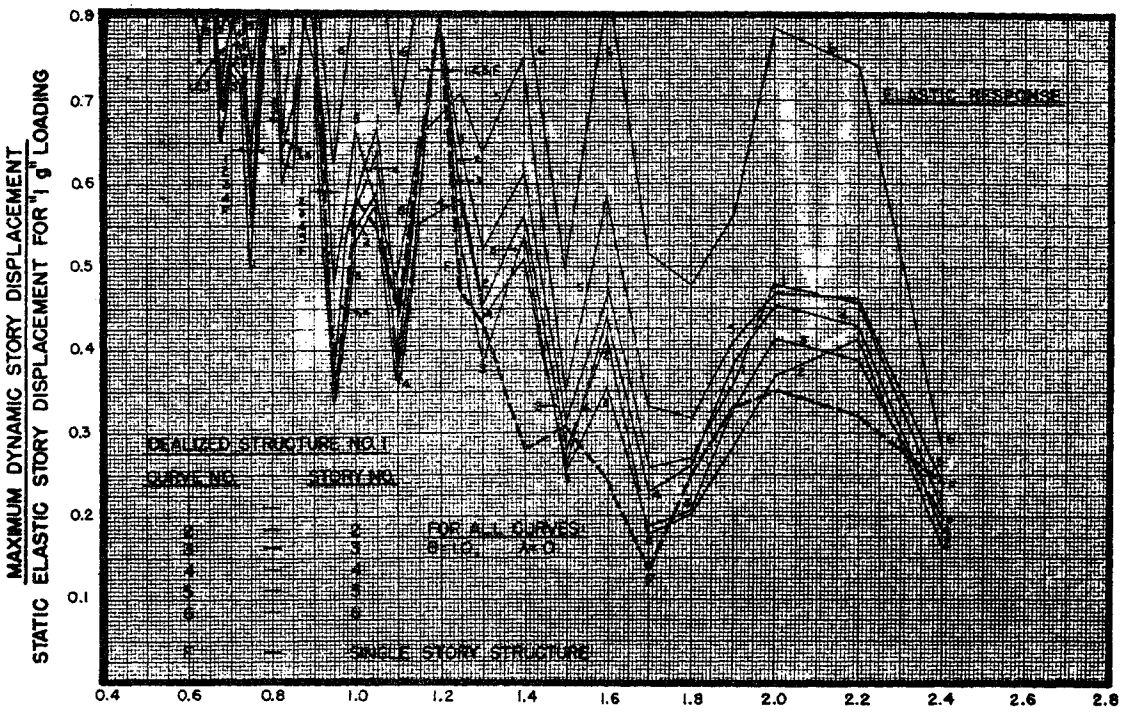

FIG. 9 -- MAXIMUM DYNAMIC RESPONSE FOR EL CENTRO, CALIFORNIA EARTHQUAKE OF MAY 18, 1940 E-W COMPONENT

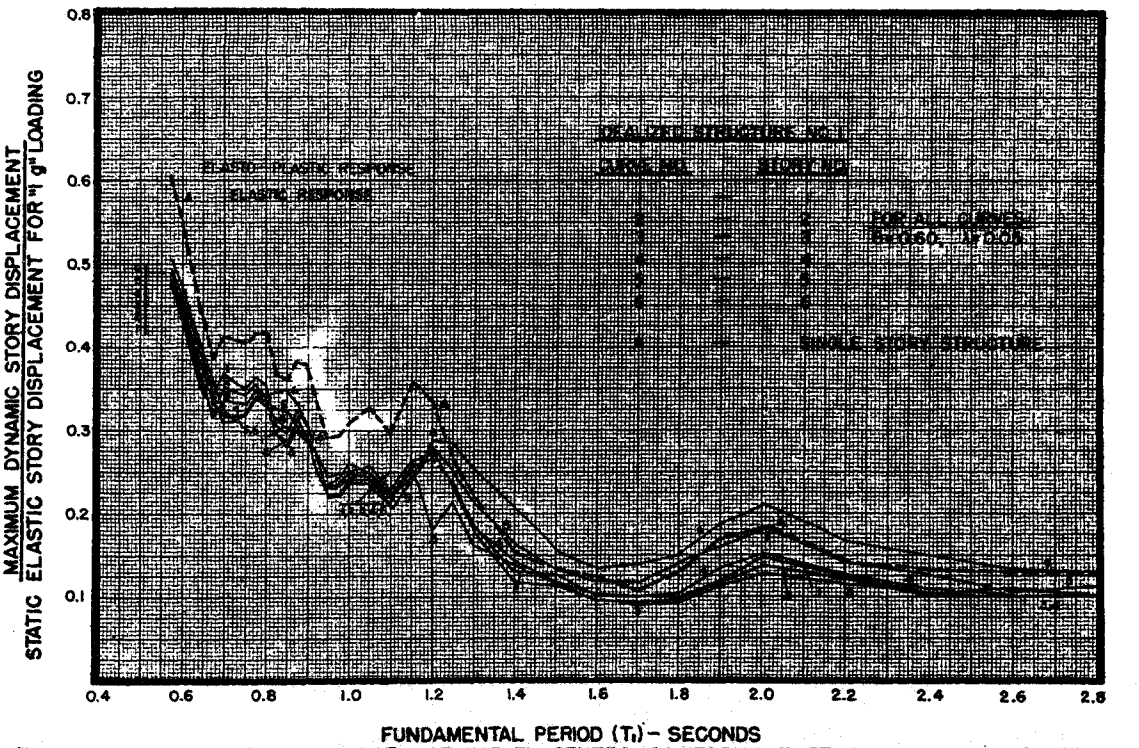

FIG. 10 -- MAXIMUM DYNAMIC RESPONSE FOR EL CENTRO, CALIFORNIA EARTHQUAKE OF MAY 18, 1940 E-W COMPONENT

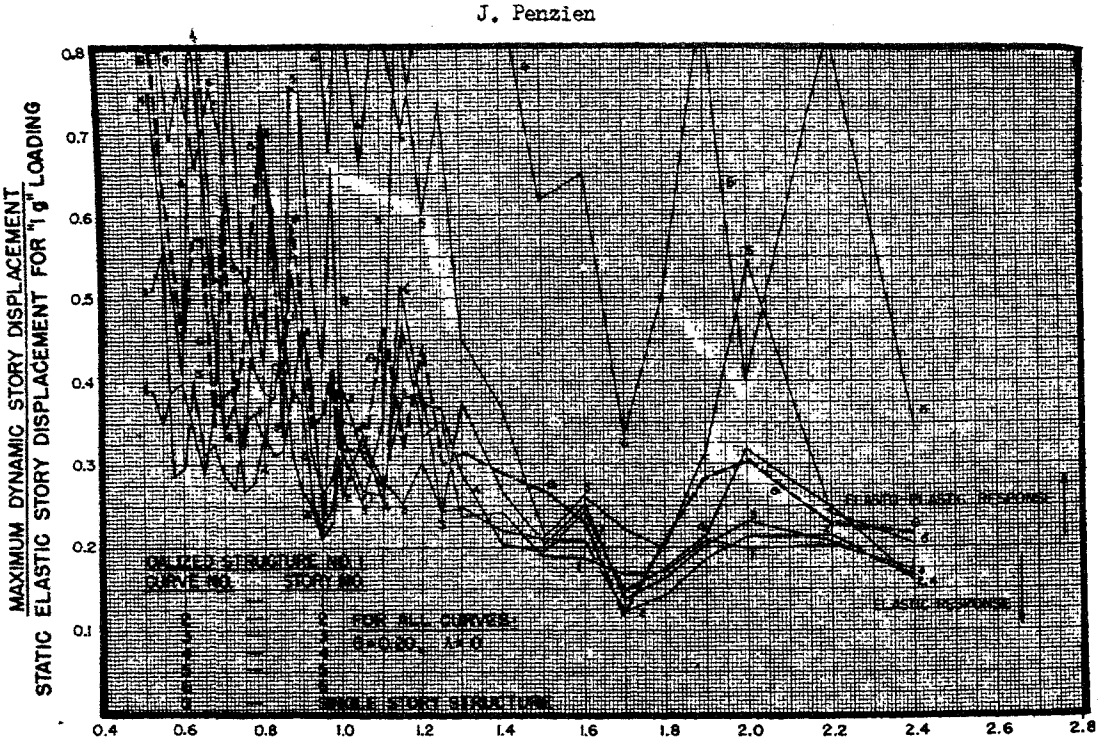

FIG. 11 -- MAXIMUM DYNAMIC RESPONSE FOR EL CENTRO, CALIFORNIA EARTHQUAKE OF MAY 18, 1940
E-W COMPONENT

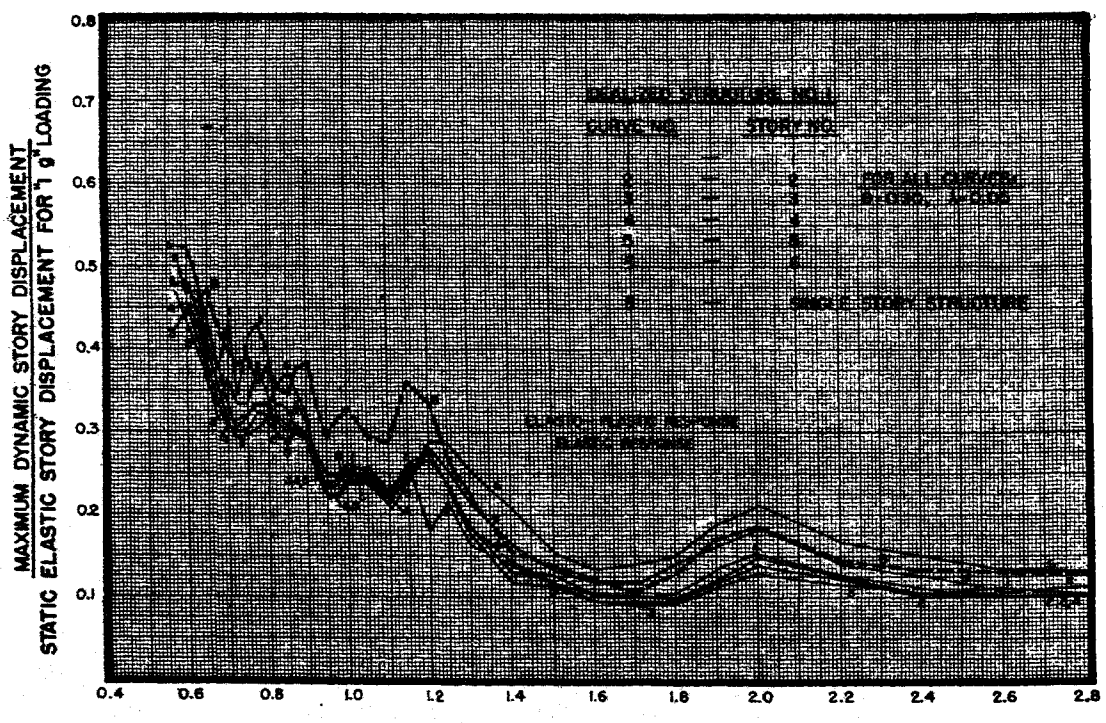

FIG. 12 -- MAXIMUM DYNAMIC RESPONSE FOR EL CENTRO, CALIFORNIA EARTHQUAKE OF MAY 18, 1940
E-W COMPONENT

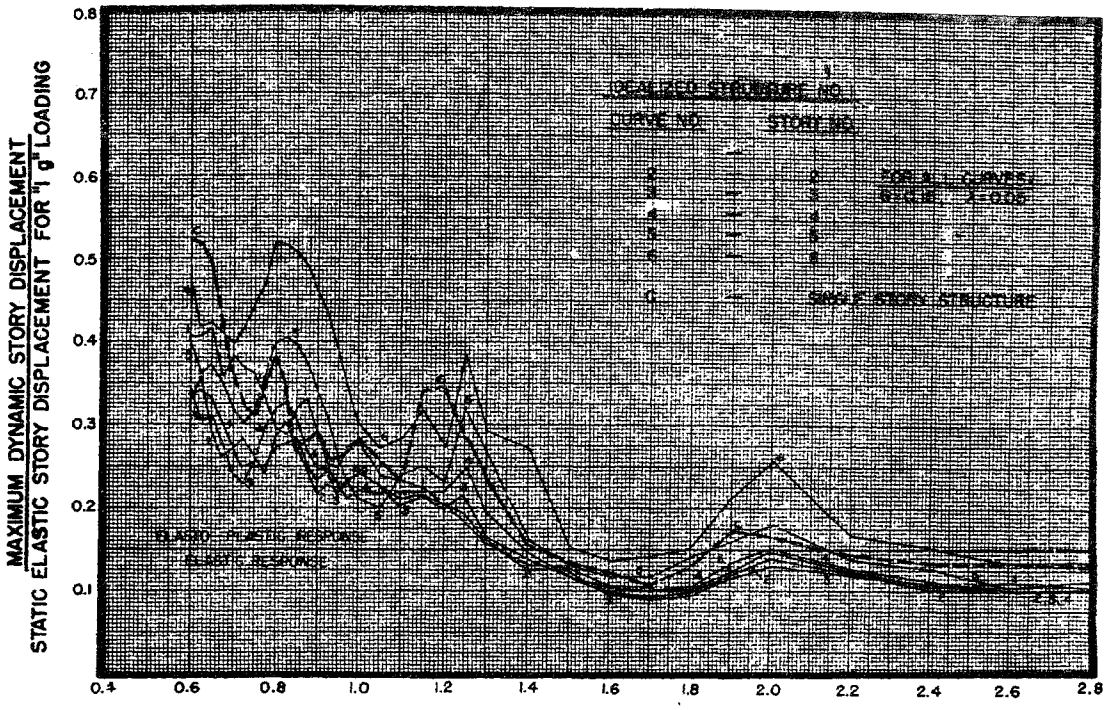

FIG. 13 -- MAXIMUM DYNAMIC RESPONSE FOR EL CENTRO, CALIFORNIA EARTHQUAKE OF MAY 18, 1940
E-W COMPONENT

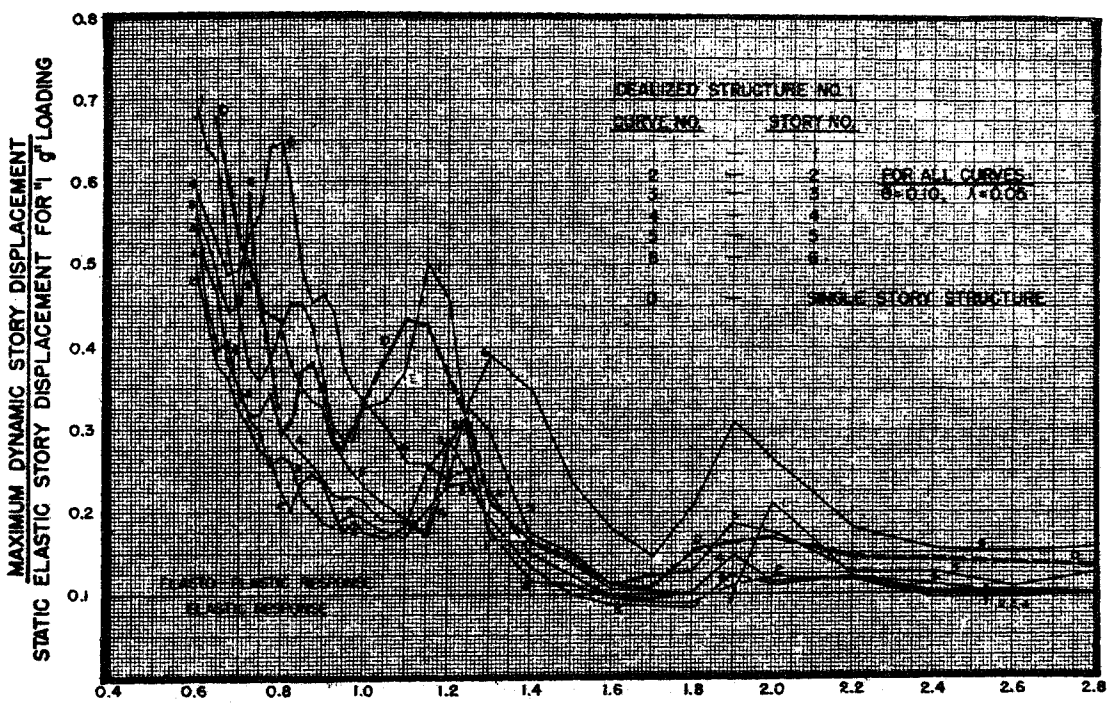

FIG. 14 -- MAXIMUM DYNAMIC RESPONSE FOR EL CENTRO, CALIFORNIA EARTHQUAKE OF MAY 18, 1940
E-W COMPONENT

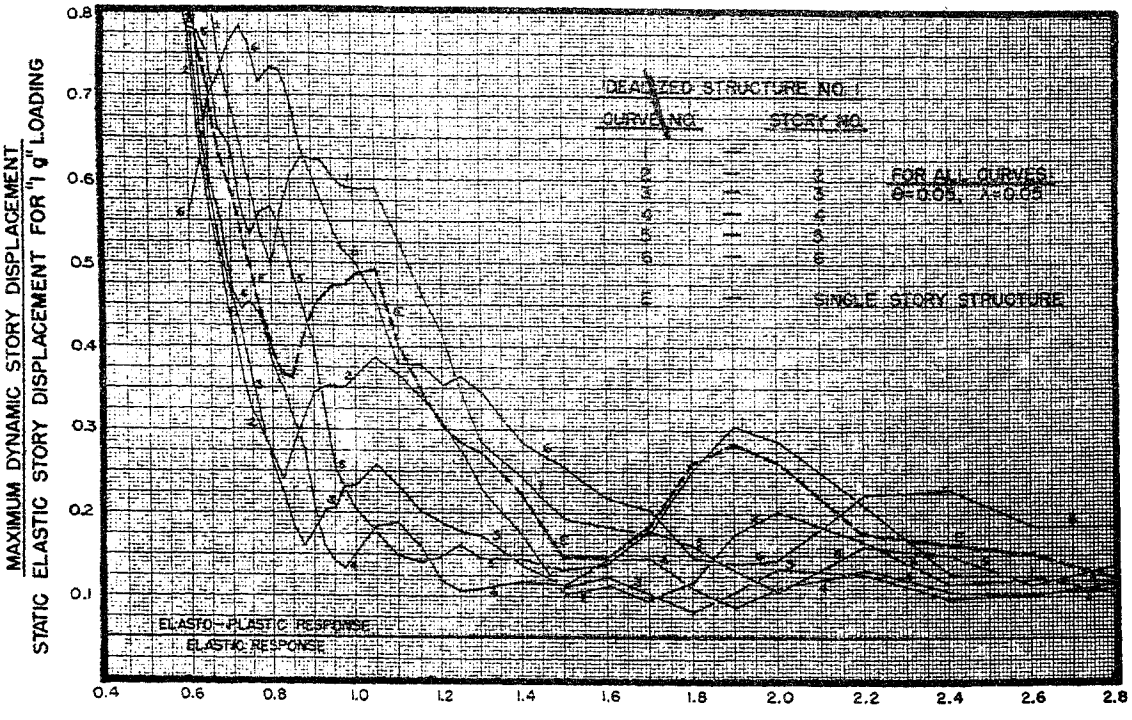

FIG. 15 -- MAXIMUM DYNAMIC RESPONSE FOR EL CENTRO, CALIFORNIA EARTHQUAKE OF MAY 18, 1940
E-W COMPONENT

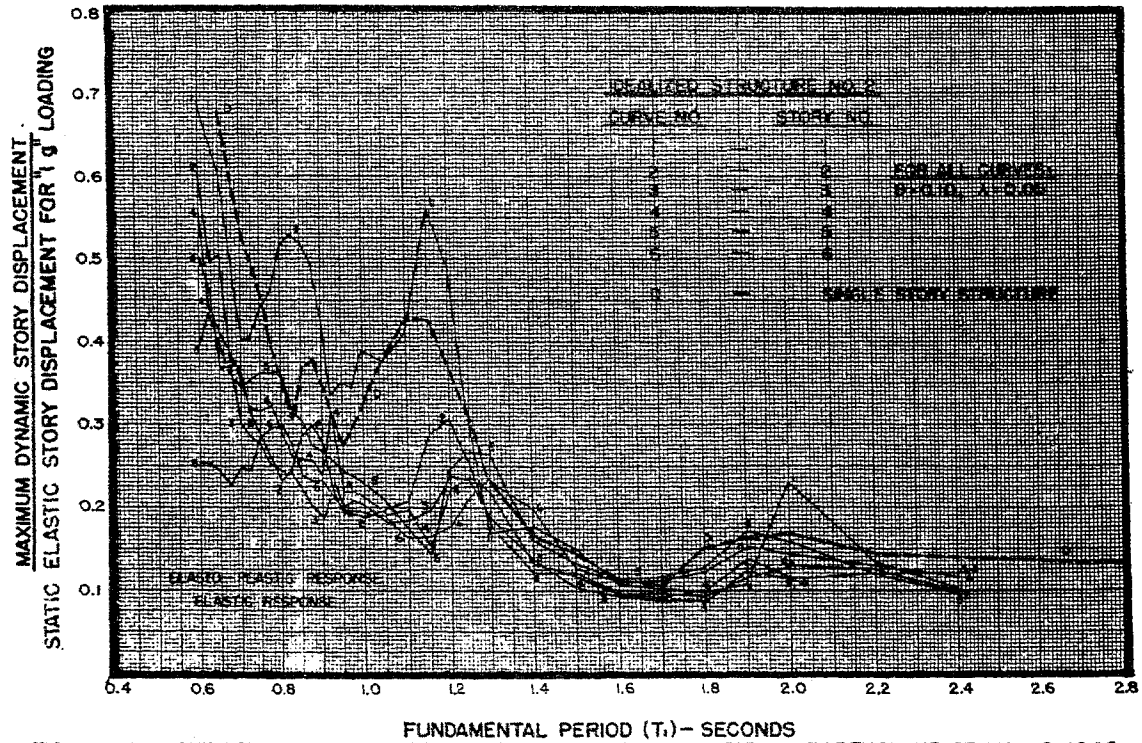

FIG. 16 -- MAXIMUM DYNAMIC RESPONSE FOR EL CENTRO, CALIFORNIA EARTHQUAKE OF MAY 18, 1940
E-W COMPONENT

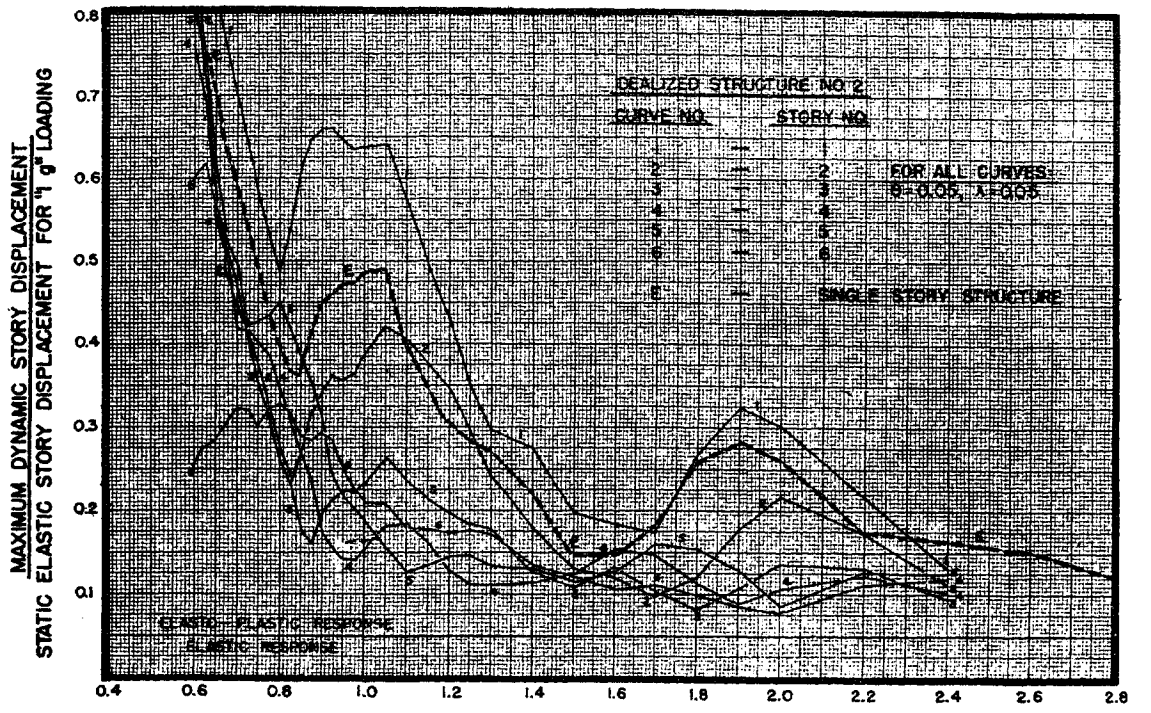

FIG. 17 -- MAXIMUM DYNAMIC RESPONSE FOR EL CENTRO, CALIFORNIA EARTHQUAKE OF MAY 18, 1940 E-W COMPONENT

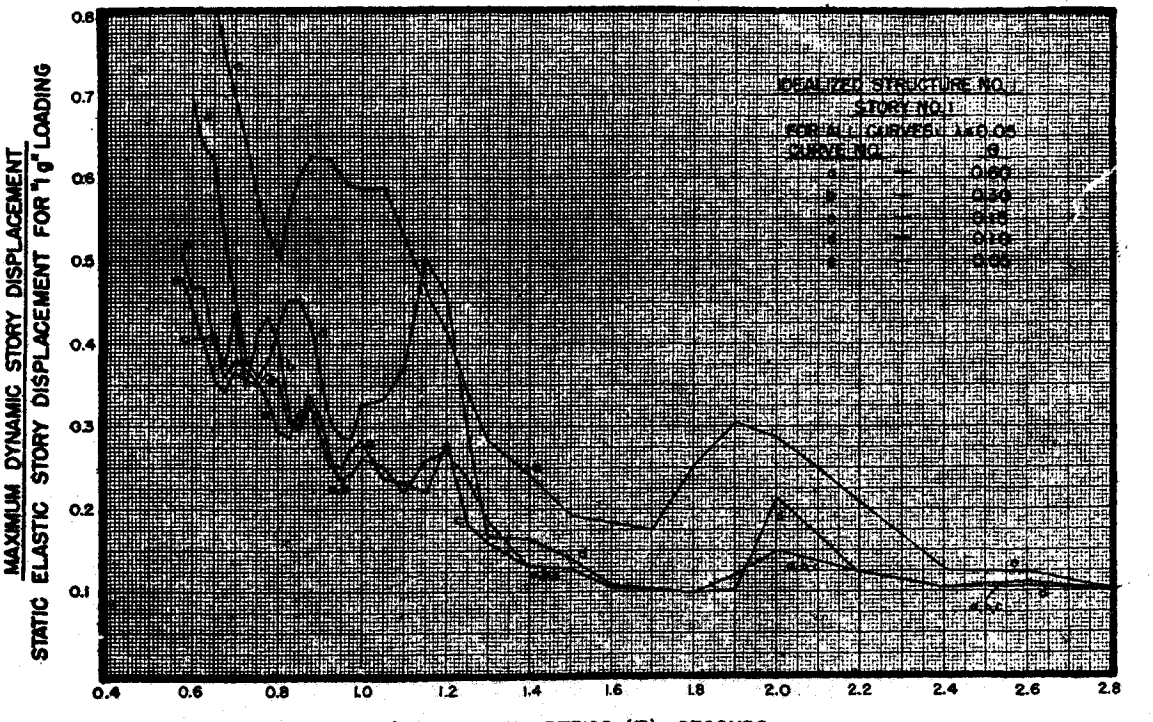

FIG. 18 -- MAXIMUM DYNAMIC RESPONSE FOR EL CENTRO, CALIFORNIA EARTHQUAKE OF MAY 18, 1940 E-W COMPONENT

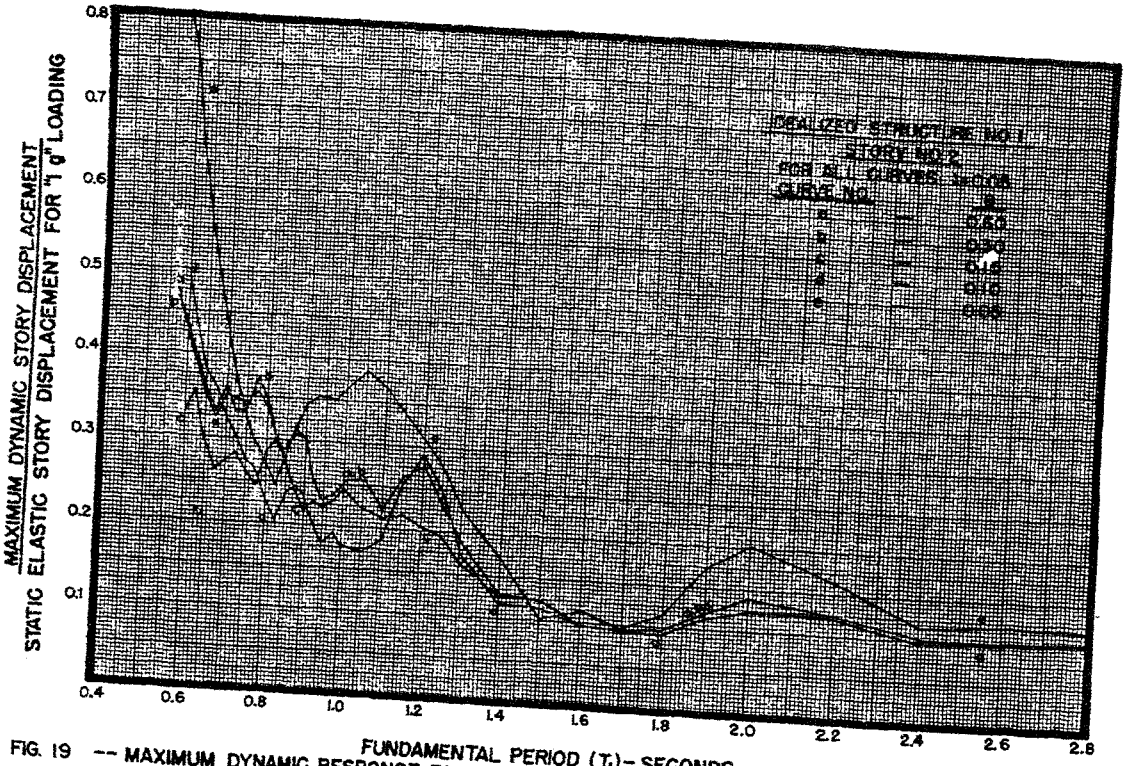

FIG. 19 -- MAXIMUM DYNAMIC RESPONSE FOR EL CENTRO, CALIFORNIA EARTHQUAKE OF MAY 18, 1940
E-W COMPONENT

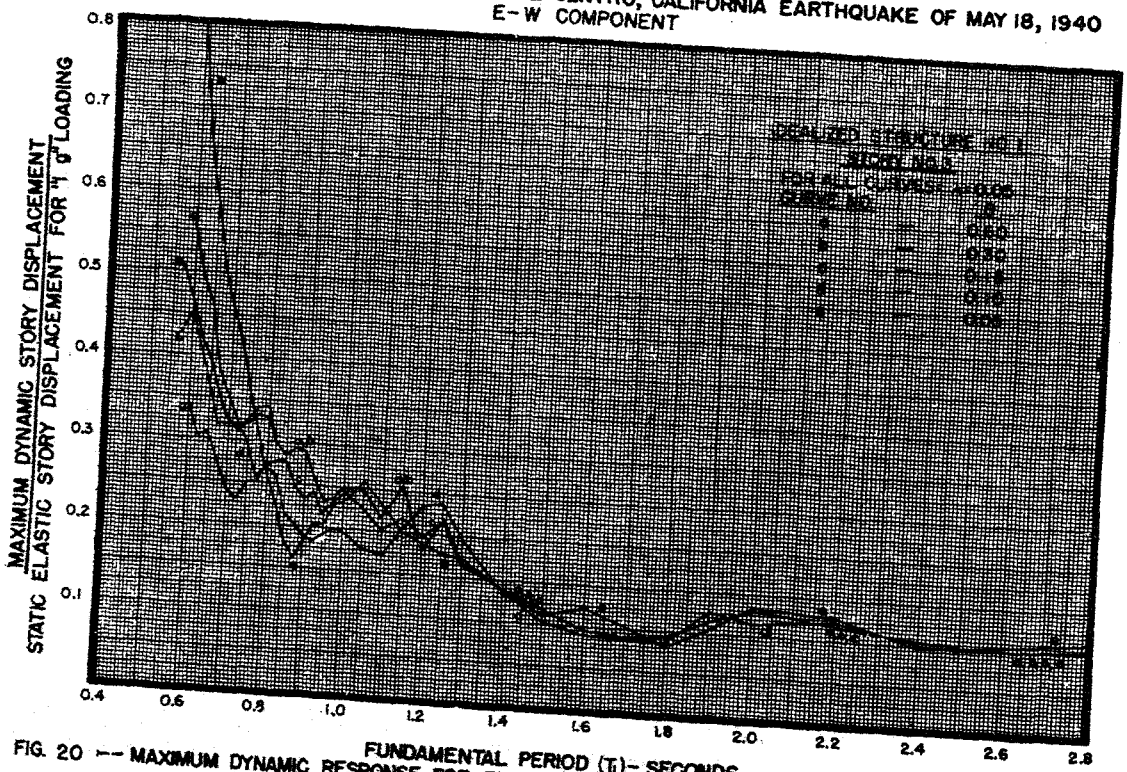

FIG. 20 -- MAXIMUM DYNAMIC RESPONSE FOR EL CENTRO, CALIFORNIA EARTHQUAKE OF MAY 18, 1940
E-W COMPONENT

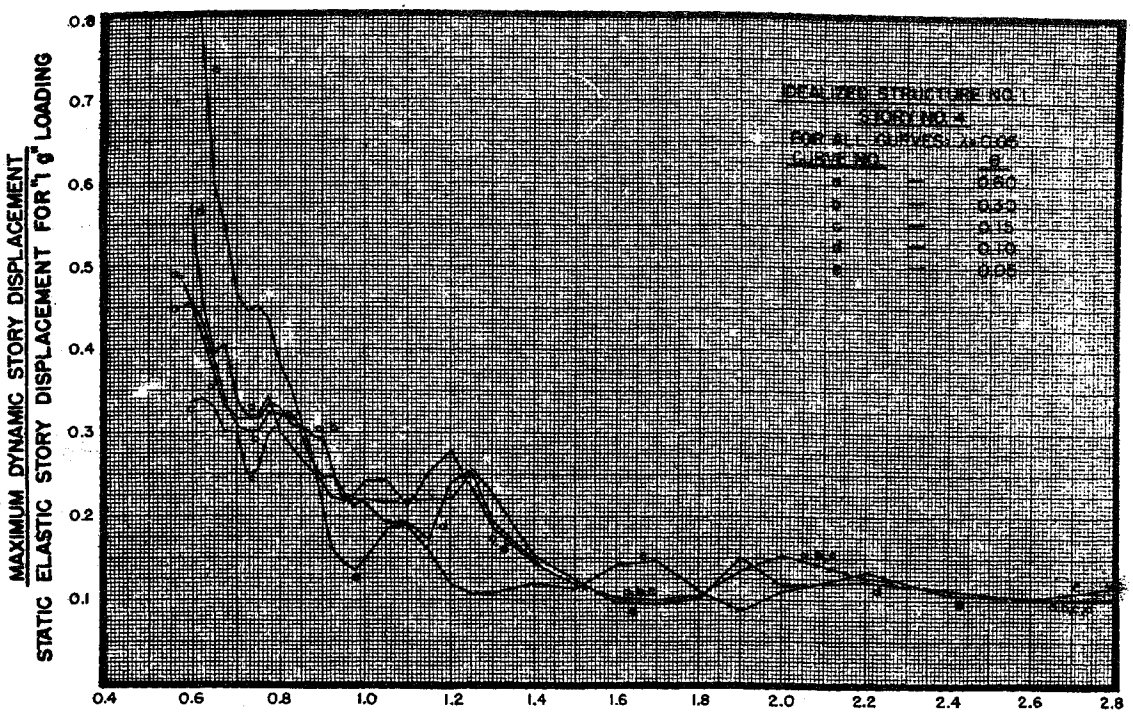

FIG. 21 -- MAXIMUM DYNAMIC RESPONSE FOR EL CENTRO, CALIFORNIA EARTHQUAKE OF MAY 18, 1940
E-W COMPONENT

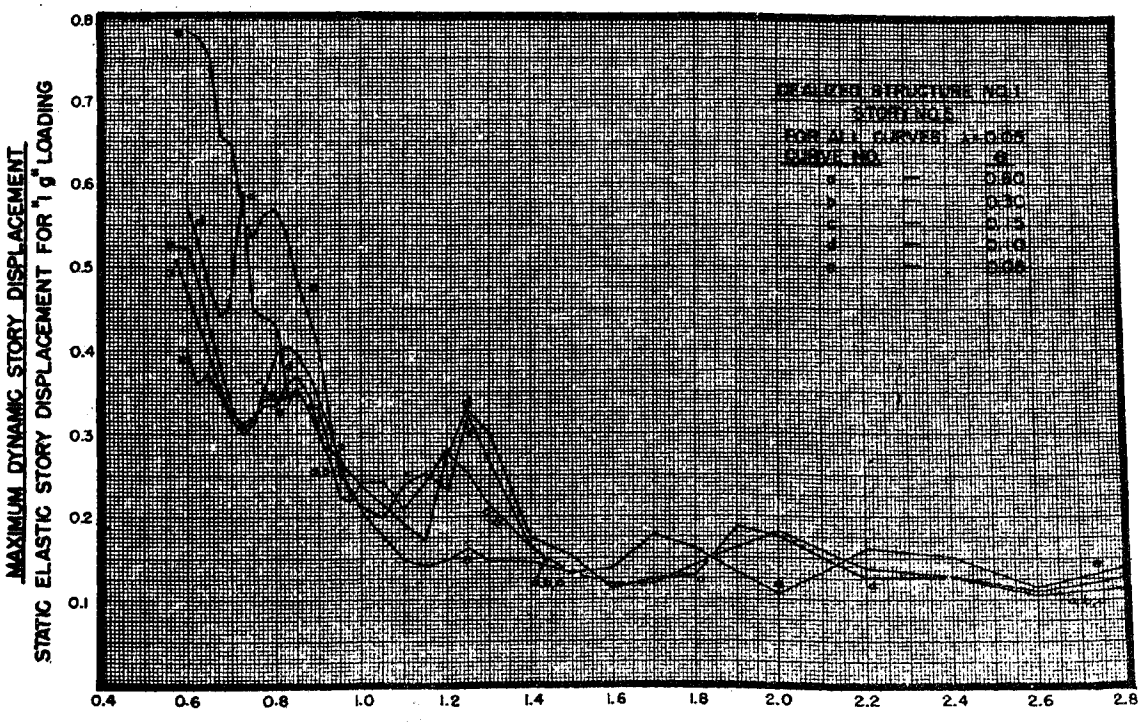

FIG. 22 -- MAXIMUM DYNAMIC RESPONSE FOR EL CENTRO, CALIFORNIA EARTHQUAKE OF MAY 18, 1940
E-W COMPONENT

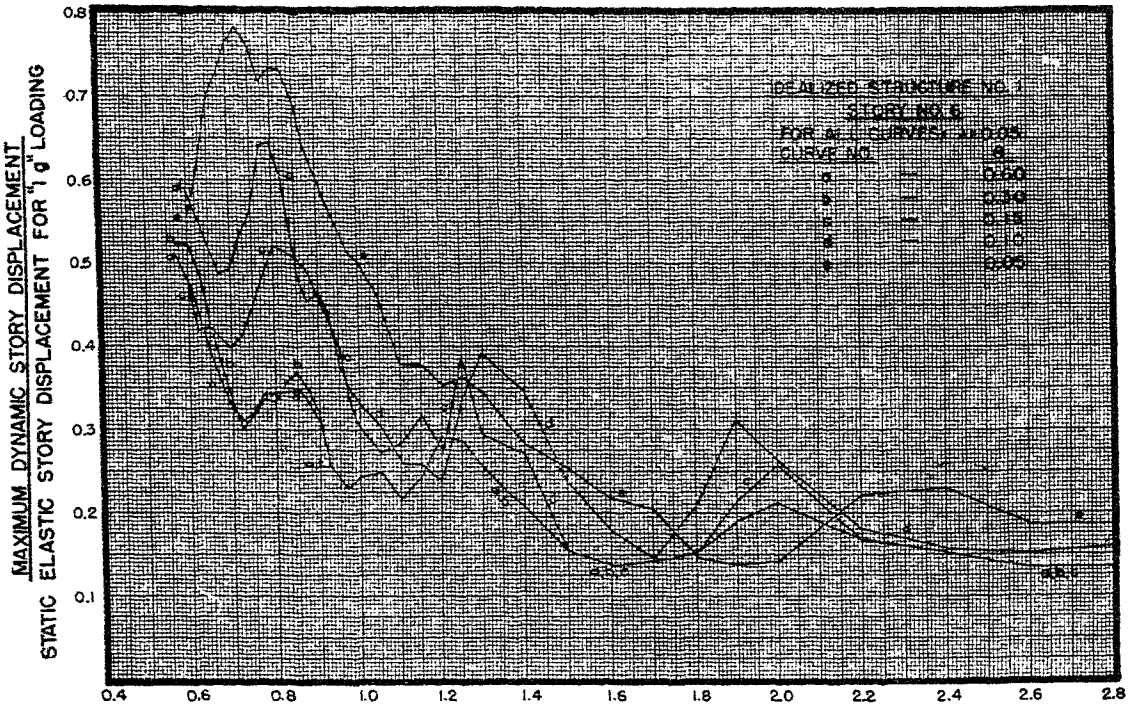

FIG. 23 -- MAXIMUM DYNAMIC RESPONSE FOR EL CENTRO, CALIFORNIA EARTHQUAKE OF MAY 18, 1940 E-W COMPONENT